Hindawi Publishing Corporation
Journal of Nanomaterials
Volume 2015, Article ID 840594, 11 pages
http://dx.doi.org/10.1155/2015/840594

Research Article

Radiosensitizing and Hyperthermic Properties of Hyaluronan Conjugated, Dextran-Coated Ferric Oxide Nanoparticles: Implications for Cancer Stem Cell Therapy

Ranjeeta Thapa,[1,2] Sandra Galoforo,[1] Sunil M. Kandel,[2] Mohammad H. El-dakdouki,[3] Thomas G. Wilson,[1] Xuefei Huang,[3] Bradley J. Roth,[2] and George D. Wilson[1]

[1]*Department of Radiation Oncology, Beaumont Health System, Royal Oak, MI 48073, USA*
[2]*Department of Physics, Oakland University, Rochester, MI 48309, USA*
[3]*Department of Chemistry, Michigan State University, East Lansing, MI 48824, USA*

Correspondence should be addressed to Ranjeeta Thapa; ranjeeta.thapa@beaumont.edu

Received 19 August 2015; Accepted 19 November 2015

Academic Editor: Piaoping Yang

Cytotoxicity, radiosensitivity, and hyperthermia sensitivity of hyaluronan-mediated dextran-coated super paramagnetic iron oxide nanoparticles (HA-DESPIONs) were assessed in CD44-expressing head and neck squamous cell carcinoma (HNSCC) cell lines at clinically relevant radiation dose and temperatures. Low-passage HNSCC cells were exposed to HA-DESPIONs and cytotoxicity was assessed using MTT assay. Radiosensitizing properties of graded doses of HA-DESPIONs were assessed in both unsorted and CD44-sorted cells using clonogenic assay in combination with 2 Gy exposure to X-rays. Hyperthermia-induced toxicity was measured at 40°C, 41°C, and 42°C using clonogenic assay. Cell death was assessed 24 hours after treatment using a flow cytometry-based apoptosis analysis. Results showed that HA-DESPIONs were nontoxic at moderate concentrations and did not directly radiosensitize the cell lines. Further, there was no significant difference in the radiosensitivity of $CD44^{high}$ and $CD44^{low}$ cells. However, HA-DESPIONs enhanced the effect of hyperthermia which resulted in reduced cell survival that appeared to be mediated through apoptosis. We demonstrated that HA-DESPIONs are nontoxic and although they do not enhance radiation sensitivity, they did increase the effect of local hyperthermia. These results support further development of drug-attached HA-DESPIONs in combination with radiation for targeting cancer stem cells (CSCs) and the development of an alternating magnetic field approach to activate the HA-DESPIONs attached to CSCs.

1. Introduction

Head and neck squamous cell carcinoma (HNSCC) is one of the leading cancers worldwide [1]. Despite advances in technologies and therapeutics such as radiation therapy, chemotherapy, and combined modality treatments, HNSCC still has a poor prognosis and survival rates have not been improved in the past few years. The heterogeneous nature of HNSCC has been demonstrated by histological, phenotypical, and karyotypical analyses [2, 3]. Although heterogeneity can be attributed to clonal evolution, there is increasing awareness that cells have significantly different abilities to proliferate and form new tumors. This has led to the hypothesis that many cancer cells have a limited ability to divide and only a small subset of phenotypically distinct cells, the cancer stem cells (CSCs), have the capacity to self-renew and form new tumors [4]. Cancer stem cells (CSCs) arise from sequential mutations in normal stem cells due to progressive genetic instability and/or environmental factors.

In HNSCC, it has been suggested that a CSC population is contained within the cell fraction that expresses high levels of CD44 [5]. CD44 is a cell surface glycoprotein and was the first cancer stem cell marker to be described in solid malignancies [6]. HNSCC cells expressing high levels of CD44 have primitive morphologic features, express high levels of the stem cell marker BMI-1, and costain with cytokeratin 5/14, a basal cell marker. In vivo, $CD44^{high}$ cells are capable of regenerating a heterogeneous tumor, whereas

Table 1: Clinicopathological characteristics of the HNSCC cell lines.

Cell line	Sex	Age (yrs)	TNM	Specimen site	Type of lesion	Grade
UT-SCC-14	M	25	$T_3N_1M_0$	Tongue	Primary	G2
UT-SCC-15	M	51	$T_1N_0M_0$	Tongue	Recurrent	G1
UT-SCC-16A	F	77	$T_3N_0M_0$	Tongue	Primary	G3
UT-SCC-24A	M	41	$T_2N_0M_0$	Tongue	Primary	G2
UT-SCC-30	F	77	$T_3N_1M_0$	Tongue	Primary	G1
UT-SCC-33	F	86	$T_2N_0M_0$	Gingiva of mandible	Primary	G2

their $CD44^{low}$ counterparts cannot [5]. Recent evidence has strengthened the potential role of CD44 in HNSCC CSCs and their influence on disease progression and treatment outcome. First, $CD44^{high}$ cells were shown to be more motile and tumorigenic than $CD44^{low}$ cells [7], and CD44 was the only biological factor which significantly correlated with response to radiotherapy in early stage larynx patients [8].

CD44 is a transmembrane protein that serves as a receptor for hyaluronan (HA) and certain matrix metalloproteinases (MMPs) [9, 10]. HA is a member of the glycosaminoglycan family and is composed of tandem disaccharide repeats of β-1, 4-D-glucuronic acid-β-1,3-D-N-acetylglucosamine [11, 12]. As an important component of extracellular matrix, HA has been shown to be directly involved in many cellular processes such as cell adhesion, cell migration, innate immunity, and wound healing [13]. Further, the association of HA-CD44 in HNSCC activates epidermal growth factor receptor (EGFR) pathways which ultimately lead to tumor cell growth, tumor cell migration, and chemotherapy resistance [14].

There is a need to develop new treatment strategies that may eventually replace traditional chemotherapy which has severe off-target side effects and unwanted toxicity [15]. Another major challenge is the development of multidrug resistance (MDR) by the tumor cells, which ultimately makes chemotherapy less effective [16–18]. Currently the use of nanoparticle systems for biological imaging and drug delivery has attracted increasing attention [19]. Of particular interest to us are dextran-coated super paramagnetic iron oxide nanoparticles functionalized with hyaluronan (HA-DESPIONs) [20]. HA immobilized on the surface of a nanocarrier (SPION) serves as an "address" molecule that is identified by a receptor molecule (in this case CD44). Hyaluronan oligosaccharides which completely inhibit HA-CD44 interaction have been shown to sensitize chemotherapy resistant lung and breast cancer cell lines [12].

In terms of using nanoparticles as enhancers of cancer treatments, it has been established that gold nanoparticles (GNPs) in combination with kilovoltage radiation can cause sensitization [21, 22], but it has yet to be established consistently whether HA-DESPIONs can radiosensitize. Although their X-ray absorption is lower than GNPs, one study has suggested that cross-linked dextran-coated iron oxide nanoparticles can result in modest radiosensitization in HeLa and EMT-6 cells [23]. In addition to radiation, hyperthermia is another treatment modality that can be generated by superparamagnetic iron oxide nanoparticles in an alternating magnetic field [24]. Hyperthermia results in the activation of many intracellular and extracellular degradation mechanisms including protein misfolding and aggregation, alteration in signal transduction, induction of apoptosis and reduced perfusion, and oxygenation of the tumor. How HA-DESPIONs interact with hyperthermia has yet to be determined.

The purpose of this study was to establish the interaction of HA-DESPIONs with radiation and hyperthermia at clinically relevant KV radiation and temperatures, respectively.

2. Materials and Methods

2.1. Cell Lines. The UT cell lines were obtained through collaboration with Dr. Reidar Grénman (University of Turku, Finland). UT-SCC-14, UT-SCC-15, UT-SCC-16A, UT-SCC-24A, UT-SCC-30, and UT-SCC-33 were developed from primary HNSCC and maintained at low-passage numbers (less than 50) such that they maintained phenotype and morphological characteristics similar to the primary tumors. The doubling times of the cells vary 48–72 hours and have plating efficiency 0.15–0.30 depending on the cell lines. The details of the cell lines information are given in Table 1. Cells were cultured in Dulbecco modified eagle/F-12 medium supplemented with 10% fetal bovine serum (FBS) and 2% of penicillin-streptomycin and maintained in incubator at 37°C with 5% CO_2/95% air. Cells were trypsinized twice before their use in any experiments.

2.2. HA-DESPION Synthesis. HA-DESPIONs were prepared as previously described [20]. Briefly, a ligand exchange reaction was utilized by creating a two-phase system where an iron oxide magnetite dispersion in tetrahydrofuran (THF) was mixed with a basic aqueous potassium hydroxide (KOH) solution of HA in the ratio of 1 : 3 w/w NP : HA. The nanoparticles have been thoroughly characterized previously by transmission electron microscopy, thermogravimetric analysis, elemental analysis, dynamic light scattering, and high-resolution magic angle spinning NMR [25, 26]. The nanoparticles used in this study had a hydrodynamic radius of 114 nm, core size of 5 nm, and a zeta potential of −47 mV. The thermogravimetric analysis data showed that HA accounted for 44% weight of each HA-DESPION.

2.3. Irradiation. Cells in 35 mm^2 dishes were irradiated (2 Gy) at 37°C with a Xstrahl X-ray System, Model RS225 (Xstrahl, United Kingdom), at a dose rate of 0.29 Gy/min, tube voltage of 160 KVp, and current of 4 mA and filtration with 0.5 mm Al and 0.5 mm Cu.

2.4. Growth Inhibition Assay. MTT (3-(4,5-dimethylthiazol-2-yl)-2, 5-diphenyltetrazolium bromide) assays were used to assess the effects of HA-DESPIONs on cell growth. Briefly, a 96-well plate was plated with cells at 3×10^3 cells/well. After 24 hours, different concentrations of HA-DESPIONs in a complete growth media (0–200 μg/mL) were added into the wells. After further 24 hours, MTT (5 mg/mL in 1x phosphate buffer saline (PBS)) was added to each well and the plate returned to the CO_2 incubator for 4-5 hours. Media containing the MTT was then aspirated from the wells and dimethyl sulfoxide (DMSO) was added to the wells to dissolve the purple formazan that formed. Following 5-minute incubation at 37°C, absorbance readings (at 560 nm and 670 nm) were taken on a VersaMax multiplate reader (Molecular Devices, Sunnyvale, CA).

2.5. Clonogenic Survival Assay. Cells were plated into 35 mm^2 culture dishes in a complete growth media and allowed to grow to 70–80% confluence. Different concentrations of HA-DESPIONs were prepared in prewarmed fresh media and added into the dishes. Four different experimental groups were set up: (1) controls, (2) 100 μg/mL HA-DESPIONs, (3) 2 Gy irradiation, and (4) 2 Gy irradiation + 1, 5, 10, 50, and 100 μg/mL HA-DESPIONs (cells were exposed to HA-DESPIONs for 24 hours prior to irradiation). Cells were irradiated at 2 Gy of single radiation dose. Immediately after the treatment, cells were allowed to rest in the incubator at 37°C for another hour, then cultured, and replated in 25 cm^2 flasks for colony formation. Colonies were allowed to develop for 10–14 days (depending on the cell lines). Colonies were stained with crystal violet stain (for an hour) and manually counted under the microscope. Survival data were obtained from 3 separate experiments for each cell line and normalized for plating efficiency (PE) by dividing the number of colonies by the number of cells plated × PE. Cell survival curves were fitted using the linear-quadratic equation.

2.6. Clonogenic Survival Assay with Sorted Cells. To establish whether differential effects might be observed based on the level of CD44 expression, cell sorting was used to isolate and study CD44^{high} and CD44^{low} cells. Freshly trypsinized cells were resuspended at 4 million cells/mL in PBS + 0.5% bovine serum albumin (BSA) and stained either with APC conjugated mouse IgG2b isotype control (BD Biosciences, San Jose, CA) or with APC-mouse antihuman CD44 IgG2b (BD Biosciences) at 8 μL/mL. After staining, cells were further washed twice with cold PBS + 0.5% BSA and resuspended in HBSS (2% FBS, 10 mM HEPES). Cells were then sorted with the BD FACSAria flow cytometer (BD Biosciences). 8×10^5 cells of both CD44^{high} and CD44^{low} were collected and plated into 35 mm^2 culture dishes at 2×10^5/dish. After overnight incubation, desired concentration of prewarmed HA-DESPIONs in freshly prepared media was added into the dishes and irradiated as (1) controls, (2) 50 μg/mL of HA-DESPIONs, (3) 2 Gy, and (4) 50 μg/mL of HA-DESPIONs and 2 Gy. After irradiation, cells were processed for the clonogenic survivals as described above.

Table 2: Growth inhibition as a function of HA-DESPION concentration in the panel of HNSCC cell lines at the two highest concentrations (100 μg/mL and 200 μg/mL). Results are presented as percent control from MTT assay.

Cell line	HA-DESPION concentration	
	100 μg/mL	200 μg/mL
UT-SCC-14	0.976 ± 0.087	0.830 ± 0.066
UT-SCC-15	0.833 ± 0.031	0.793 ± 0.023
UT-SCC-16A	0.865 ± 0.030	0.787 ± 0.042
UT-SCC-24A	0.862 ± 0.080	0.763 ± 0.071
UT-SCC-30	0.811 ± 0.080	0.776 ± 0.071
UT-SCC-33	0.942 ± 0.083	0.839 ± 0.055

2.7. Hyperthermic Activation of HA-DESPIONs. Two different cell lines (UT-SCC-14 and UT-SCC-15) were used for hyperthermia studies. Cells were plated at 2×10^5/dish in 35 mm^2 dishes and allowed to grow for two days. The media of the dishes was replaced with prewarmed media with or without 100 μg/mL of HA-DESPIONs and placed in a circulating water bath for hyperthermia treatment for 2 hours at 37°C, 40°C, 41°C, or 42°C. Immediately after hyperthermia treatment, cells were processed for clonogenic survival. Each experiment was repeated twice. In addition, cells were sorted for CD44 expression, as previously described, and the preceding experimental protocol repeated for CD44^{high} and CD44^{low} cells.

2.8. Apoptosis Analysis. To study apoptosis after hyperthermia, cells were allowed to rest in the incubator at 37°C for 24 hours after hyperthermia treatment in order to undergo apoptotic cell death. Cells were trypsinized, counted, washed in cold PBS solution, stained with the appropriate concentrations of FITC-Annexin V apoptosis detection reagents (BD Biosciences), and analyzed on a FACSCanto II flow cytometer (BD Biosciences).

2.9. Statistical Analysis. Data was expressed as mean ± SD and analyzed using Student's t-test. A P value ≤ 0.05 was considered to be statistically significant.

3. Results

3.1. The Effect of HA-DESPIONs on Cell Growth. Different concentrations (0, 10, 25, 50, 75, 100, and 200 μg/mL) of HA-DESPIONs solution, made in a complete growth media or serum free media, were tested to observe cellular growth inhibition in the panel of cell lines. The data for each concentration ($n = 8$) were averaged and normalized to the nontreated cells (control) averaged data. Figures 1(a) and 1(b) show data for the UT-SCC-14 and UT-SCC-15 cell lines which show modest growth inhibition at the higher concentrations. A similar result was found with the entire cell lines tested which is shown in Table 2.

3.2. The Effect of HA-DESPIONs on Radiosensitivity: Unsorted Cells. Clonogenic assays were performed on unsorted

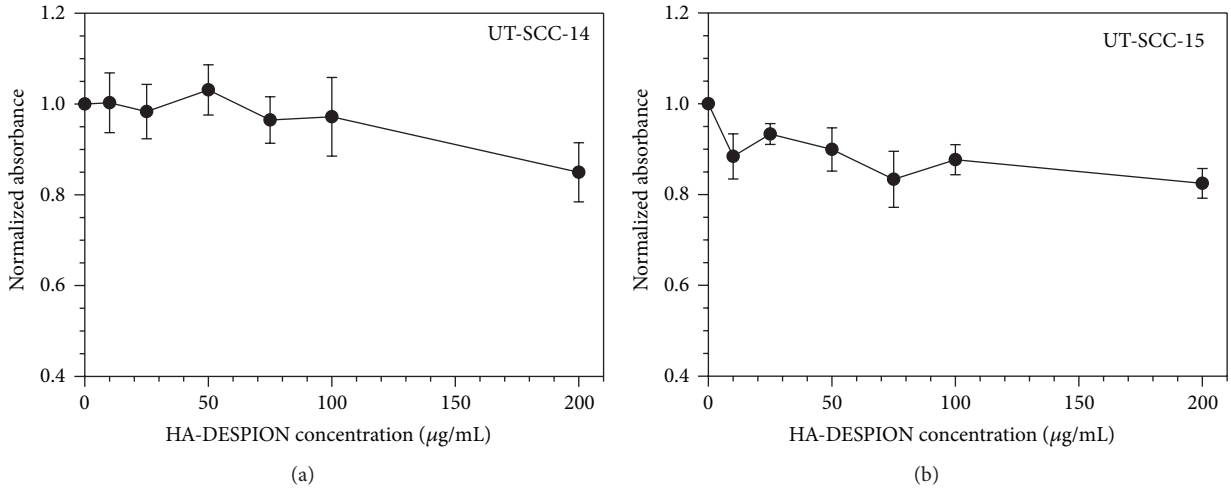

Figure 1: Dose response of growth inhibition by HA-DESPIONs in UT-SCC-14 (a) and UT-SCC-15 (b) cells.

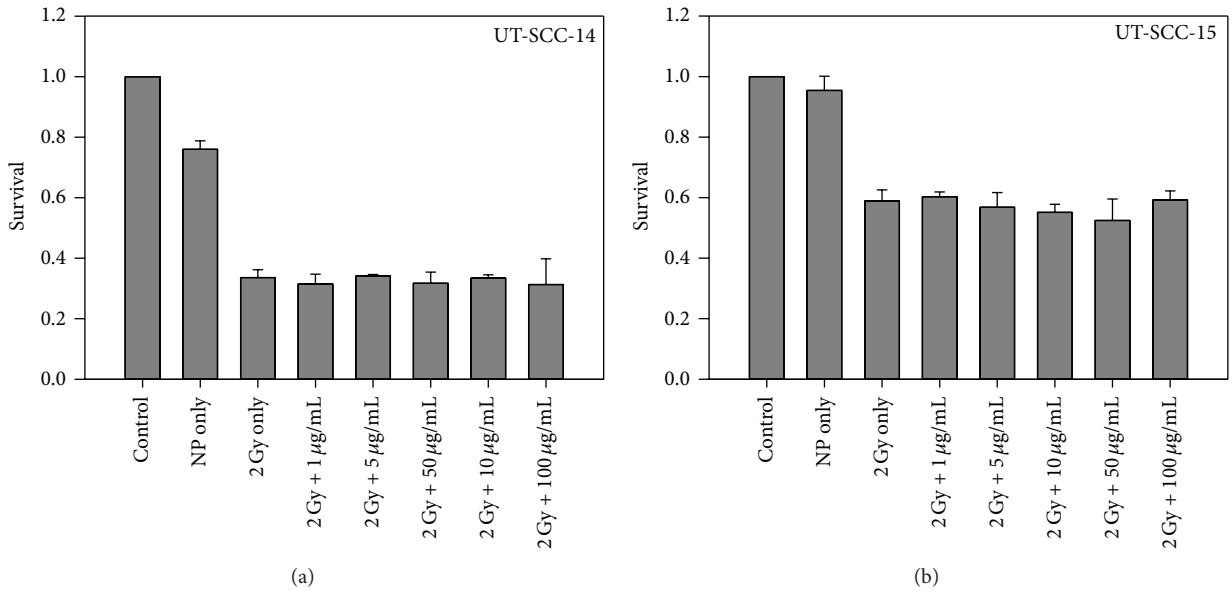

Figure 2: Effect of HA-DESPIONs in combination with 2 Gy of radiation on cell survival in unsorted UT-SSC-14 (a) and UT-SCC-15 (b) cells.

UT-SCC cells using a radiation dose of 2 Gy which generally causes a 40–70% reduction in cell survival in these cell lines. It can be seen from representative data in Figure 2 that differing concentrations of HA-DESPIONs up to 100 μg/mL had no effect on radiation sensitivity. This effect was observed in all 6 cell lines that were tested (Table 3).

3.3. The Effect of HA-DESPIONs on Radiosensitivity: CD44 Sorted Cells. To determine if a differential effect might be associated with cells expressing high levels of CD44 compared to cells with low levels, cell sorting was used to isolate these cell populations and repeat the radiosensitivity assessment. A CD44 sort was performed on the BD FACSAria flow cytometer. Figure 3 shows cell survival data in all six representative cell lines, (a) UT-SCC-14, (b) UT-SCC-15, (c) UT-SCC-16A, (d) UT-SCC-24A, (e) UT-SCC-30, and (f) UT-SCC-33. There was no significant difference of radiosensitivity between the $CD44^{high}$ and $CD44^{low}$ cells in any of these cell lines.

Table 3: The effect of HA-DESPION at low (10 μg/mL) and high (100 μg/mL) concentrations along with 2 Gy of radiation in the panel of UT-SCC cell lines.

Cell line	HA-DESPION concentration	
	10 μg/mL	100 μg/mL
UT-SCC-14	0.317 ± 0.037	0.313 ± 0.085
UT-SCC-15	0.552 ± 0.027	0.592 ± 0.030
UT-SCC-16A	0.482 ± 0.017	0.437 ± 0.007
UT-SCC-24A	0.354 ± 0.032	0.366 ± 0.012
UT-SCC-30	0.448 ± 0.021	0.429 ± 0.021
UT-SCC-33	0.602 ± 0.036	0.600 ± 0.018

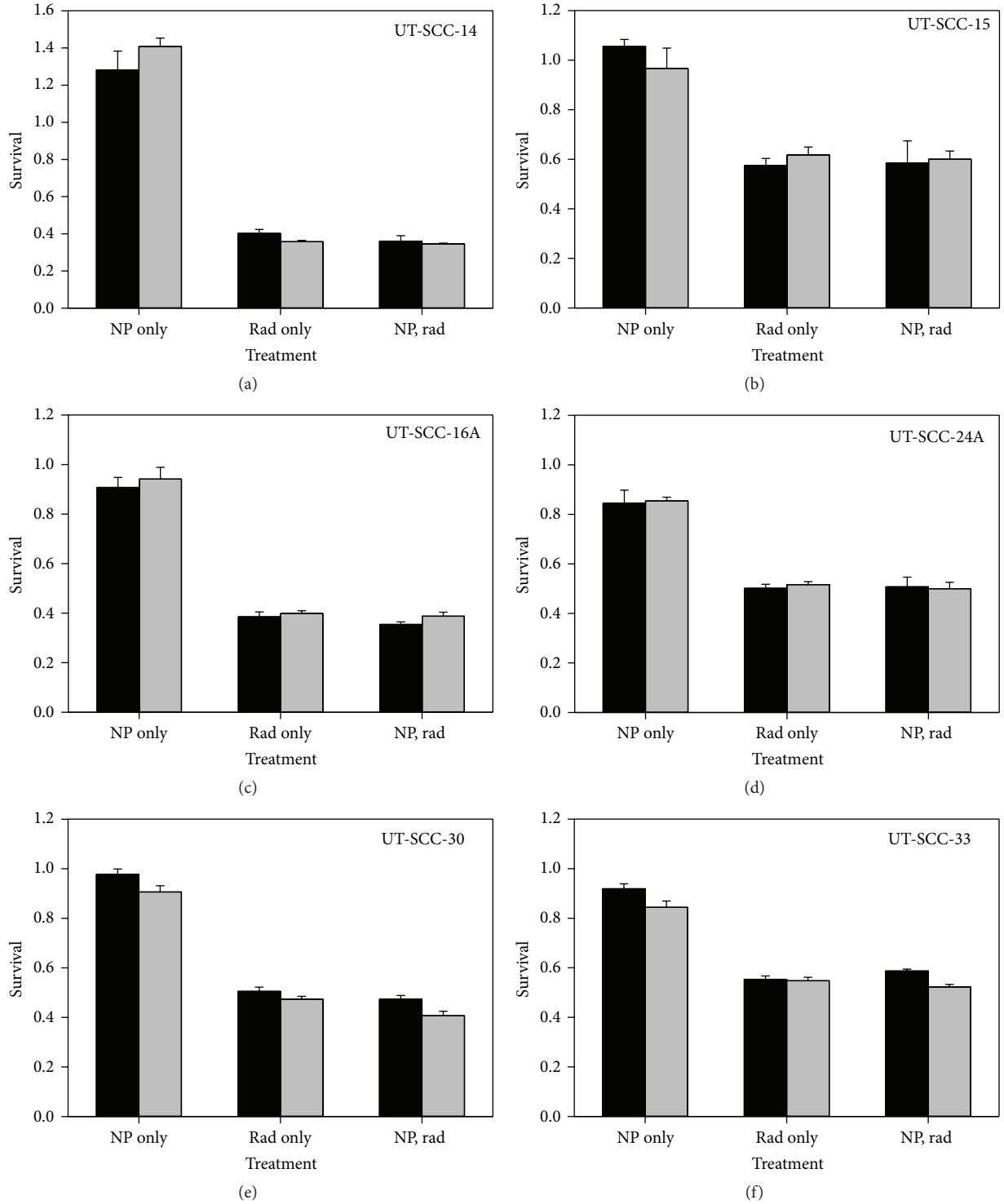

Figure 3: Effect on cell survival of HA-DESPIONs in combination with 2 Gy irradiation in $CD44^{high}$ (black column) and $CD44^{low}$ (gray column) sorted cells of UT Cell lines; (a) UT-SSC-14, (b) UT-SCC-15, (c) UT-SCC-16A, (d) UT-SCC-24A, (e) UT-SCC-30, and (f) UT-SCC-33 cells.

3.4. Hyperthermia Sensitivity of the UT Cell Lines. Having established a favorable toxicity profile of the HA-DESPIONs and demonstrated that there is no direct radiosensitizing effect of the NPs, we next investigated the interaction with hyperthermia. In order to determine the appropriate heating time for hyperthermic treatment, UT cell lines were heated for 0–3 hours at different temperatures. The effect of heat (Figure 4) was cell line dependent. There was a modest reduction in cell survival at 40°C or 41°C in the UT-SCC-14 and UT-SCC-15 cells which was not statistically significant.

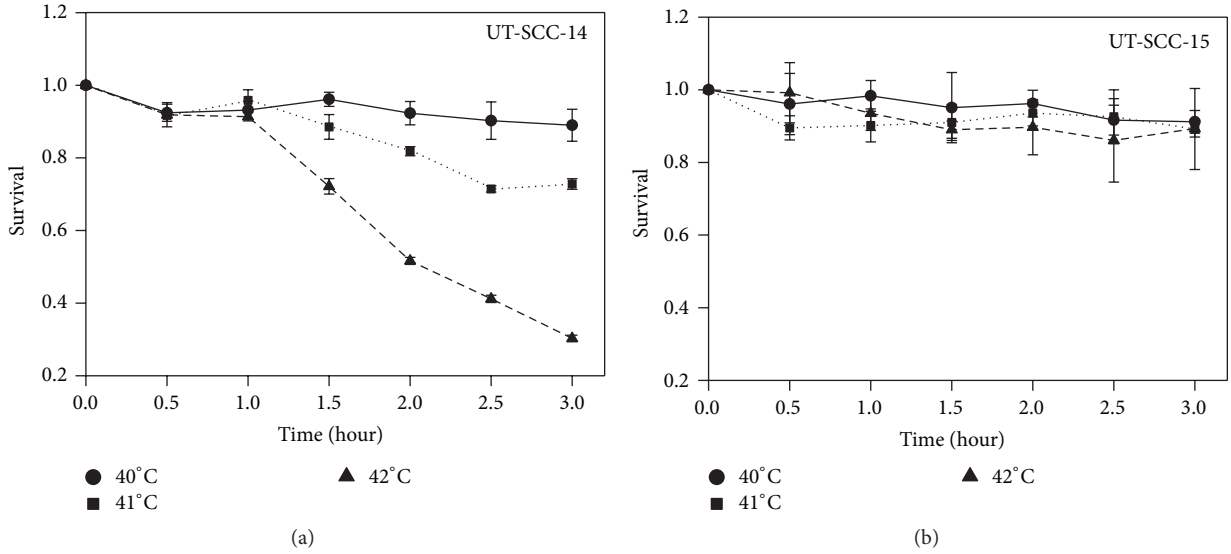

Figure 4: Hyperthermic sensitivity of (a) UT-SCC-14 and (b) UT-SCC-15 cells. The data are presented for 40°C (—), 41°C (- - - -), and 42°C (– · – · –).

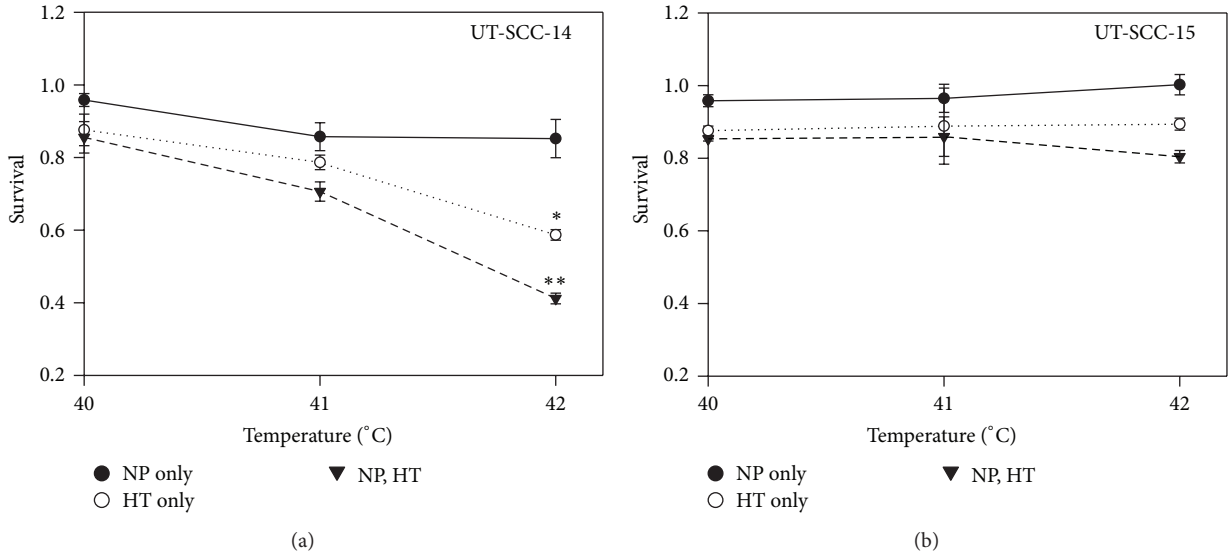

Figure 5: Effect of HA-DESPIONs on hyperthermic sensitivity in unsorted UT-SCC-14 (a) and UT-SCC-15 (b) cells. The data are presented for 40°C (—), 41°C (- - - -), and 42°C (– · – · –). There was significant effect ($P = 0.0121$) when the HA-DESPIONs were combined with hyperthermia at 42°C for 2 hours compared with any of the single treatments.

However, 2-hour exposure to 42°C resulted in 50% reduction in cell survival in UT-SCC-14 cells but only 10–15% reduction in UT-SCC-15 cells.

3.5. Effect of HA-DESPIONs on Hyperthermic Sensitivity in UT-SCC-14 and UT-SCC-15 Cells. In Figure 5(a), UT-SCC-14 cells treated with 100 μg/mL of HA-DESPIONs at 37°C resulted in about 5–10% of growth inhibition. The combined effects of hyperthermia at 40°C or 41°C with the HA-DESPIONs did not produce a significantly greater amount of cell killing than either agent alone. However, there was significant effect ($P = 0.0121$) when the HA-DESPIONs were combined with hyperthermia at 42°C for 2 hours compared with any of the single treatments. In Figure 6, the experiment was repeated using sorted $CD44^{high}$ and $CD44^{low}$ cells. Again, there was no significant difference between $CD44^{high}$ and $CD44^{low}$ cells when exposed to HA-DESPIONs at 40°C and 41°C (Figures 6(a) and 6(b)). The sorted cells were more sensitive than unsorted cells to exposure to hyperthermia at 42°C, but there was no significant difference between the $CD44^{high}$ and $CD44^{low}$ sorted populations (Figure 6(c)). A similar result was found with UT-SCC-15 cells, which were less sensitive to hyperthermia at all temperatures compared to UT-SCC-14 cells (Figure 5(b)), but also did not show a significant additive effect in either unsorted or sorted cell populations (Figures 5(b), 6(d), 6(e), and 6(f)).

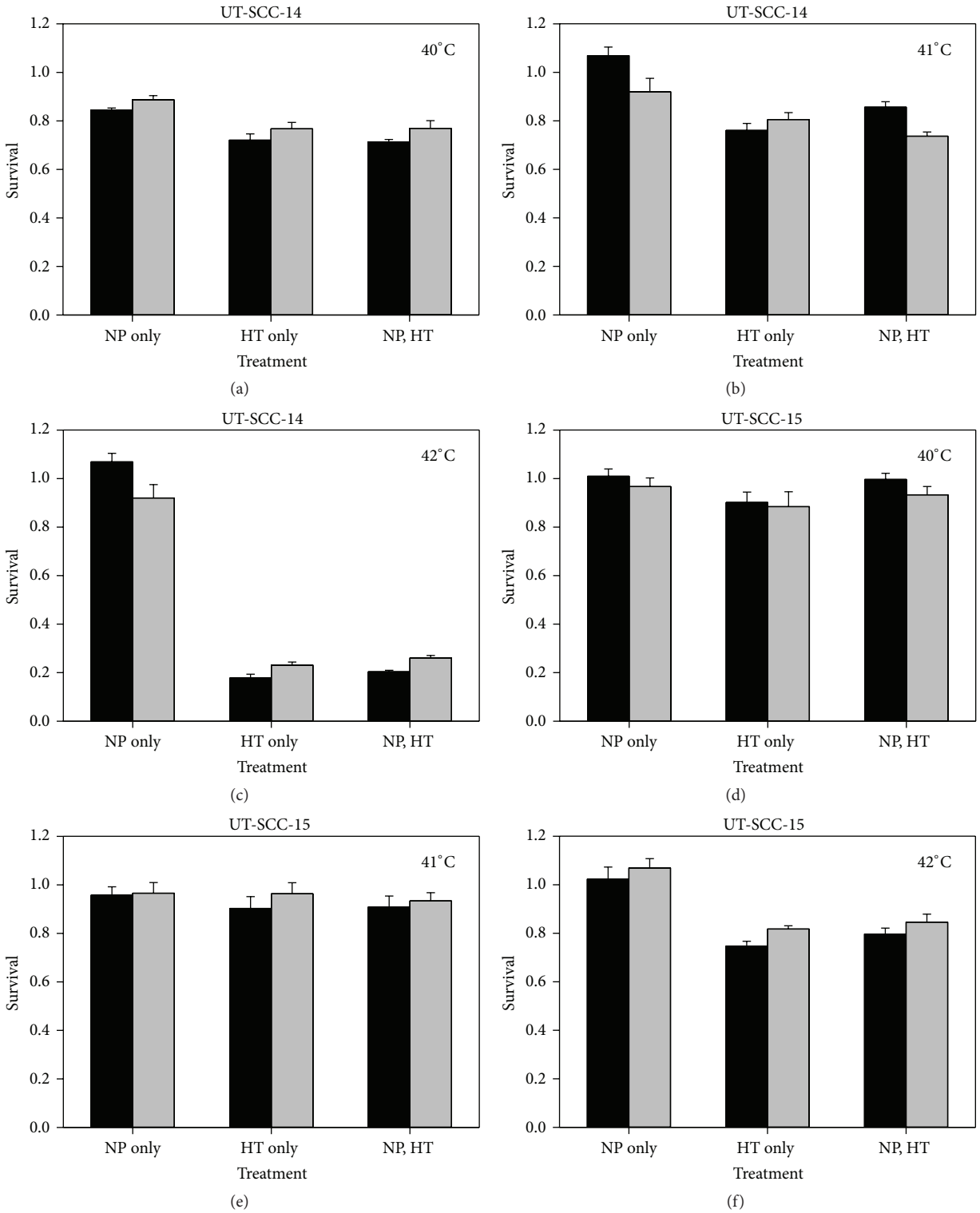

Figure 6: Effect of HA-DESPIONs on hyperthermic sensitivity in $CD44^{high}$ (black column) and $CD44^{low}$ (gray column) cells. The data are presented for UT-SCC-14 cells at 40°C (a), 41°C (b), and 42°C (c) and for UT-SCC-15 cells at 40°C (d), 41°C (e), and 42°C (f).

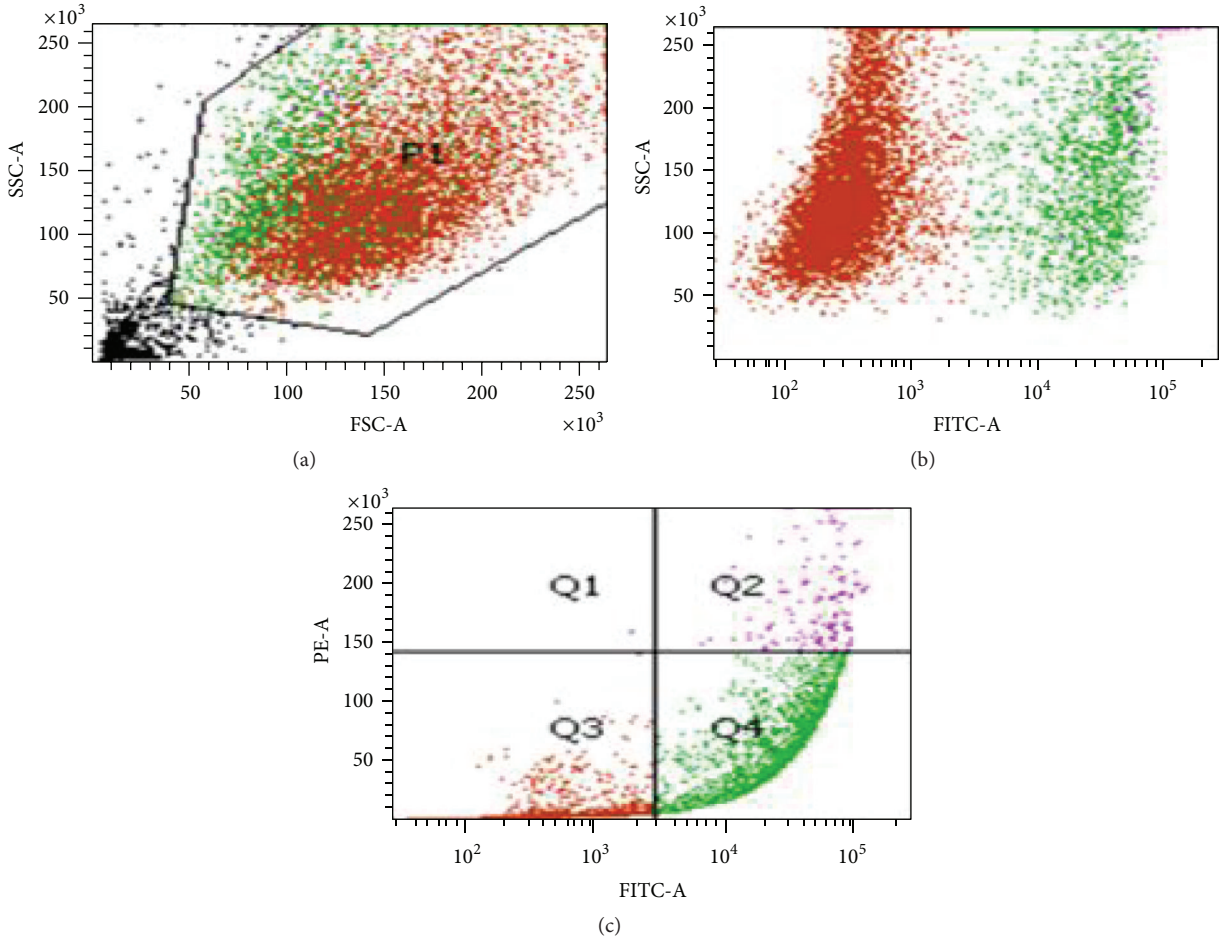

Figure 7: Detection of apoptotic cells with Annexin V. The cell population was gated on forward and side scatter (a); the apoptotic population was clearly separated from the nonapoptotic cells in the side scatter/FITC dot plot (b). Quadrant analysis (c) was used to discriminate intact cells (quadrant 3) from apoptotic cells (quadrant 4) and necrotic cells (quadrant 2).

3.6. Induction of Apoptosis in Response to HA-DESPIONs and Hyperthermia . Annexin V staining was used to identify apoptosis immediately after treatments and at 24 hours after treatment (Figure 7). Control cells consistently exhibited a background level of apoptosis between 8 and 10%. Addition of nanoparticles to cells at 37°C had no effect on apoptosis. Incubating cells at 40°C or 41°C also failed to increase apoptosis levels in UT-SCC-14 and UT-SCC-15 cells. However, incubation at 42°C did increase apoptosis levels by approximately 30% (Figure 8). Addition of nanoparticles to hyperthermic treatment at 40°C or 41°C had no effect on apoptosis. The most significant increase ($P = 0.0375$) in apoptosis was observed when nanoparticles were combined with hyperthermia at 42°C in which apoptotic levels rose to 16% representing a 1.7 ± 0.1-fold increase compared to controls.

4. Discussion

Iron oxide nanoparticles present many interesting qualities that can be exploited in MRI imaging and as drug carriers and enhancers of cancer therapy. Previous work using the HA-DESPIONs has shown that they retained the native biological recognition of HA receptor CD44 [25]. As previously discussed, CD44 is an established marker of cancer stem cells in head and neck cancer [27] and is a promising target for a variety of anticancer therapeutic approaches [12]. In this study we examined the cytotoxic profile of HA-DESPIONs alone and in combination with radiation and hyperthermia and whether differential effects were evident based on CD44 expression levels.

Initial studies showed that HA-DESPIONs are nontoxic to cells at moderate concentrations and do not directly radiosensitize HNSCC tumor cells. Nanoparticle-mediated radiosensitization has mainly been the domain of gold-based nanoparticles due to their high atomic number ($Z = 79$) which results in emissions of scattered X-rays/photons, photoelectrons, Compton electrons, Auger electrons, and fluorescence photons due to interaction between X-rays and the metal [28]. The X-ray absorption of iron oxide nanoparticles is lower than gold-based nanoparticles with an absorption factor of 1.2 [29] and although some studies have demonstrated an interaction with radiation [23], these enhancements have been relatively modest and thought to

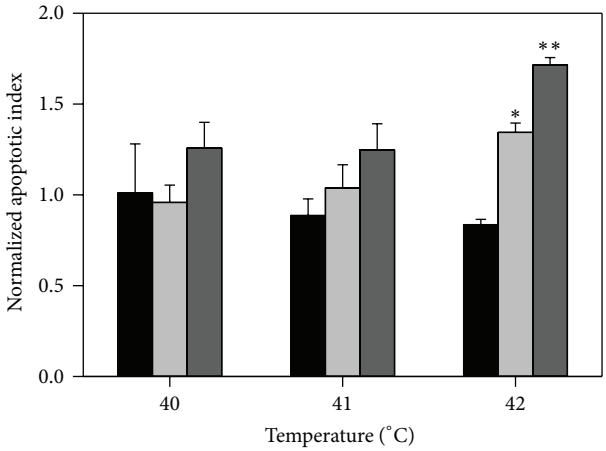

Figure 8: The apoptotic response of HA-DESPIONs in combination with hyperthermia in UT-SCC-14 cells. The normalized apoptotic index (relative to controls) is presented at three different temperatures for nanoparticles alone (black column), hyperthermia alone (gray column), and the combination of hyperthermia and nanoparticles (dark gray column). Nanoparticles combined with hyperthermia at 42°C showed significant growth in apoptotic cell death compared to any other combinations ($P = 0.0375$).

be manifested through enhanced reactive oxygen species formation [30, 31]. Previous work has shown that the HA coating of the HA-DESPIONs significantly improves receptor mediated transcytosis through CD44 binding resulting in tandem cycles of endocytosis and exocytosis [32]. This recycling of CD44 receptors between the cell surface and interior of the cell increases tumor penetration of the nanoparticles. However, this did not translate into an interaction with radiation at the level of DNA damage in this present study. This lack of radiosensitization was also absent in cells that were enriched for the highest expression levels of CD44 using a cell sorting approach.

The HA-DESPIONs used in this study have previously been shown to be detectable in tumors and atherosclerotic plaques using static magnetic fields to provide contrast for magnetic resonance imaging [11, 33]. This is because stabilized superparamagnetic iron oxide nanoparticles are characterized by inherently high T2/T2* relaxivity causing strong local inhomogeneities which can be detected as hypointense areas. Another potential application of nanoparticles based on ferric oxide is their ability to produce heat in response to appropriate alternating magnetic fields (AMF). This area of research has great potential in cancer hyperthermia treatment and has been explored clinically with mixed success due to biophysical limitations [34, 35]. Although superparamagnetism may not be an ideal attribute for activation in an AMF due to its lack of hysteresis [36], we were interested in studying this effect as a recent study addressed this issue and found modest hyperthermia-favorable characteristics (specific loss power (SLP)) in SPIO-based nanoparticles [37]. In this study, we found that physical hyperthermia enhanced the effect of HA-DESPIONs resulting in evident growth inhibition and triggering of apoptotic cell death. However, the activation was cell line dependent and was not synergistic unless a temperature of 42°C was applied; synergy was only evident in the UT-SCC-14 cells and not in the UT-SCC-15 cell line where additive effects were observed at all temperatures.

Cell survival was reduced to approximately 50% when UT-SCC-14 cells were exposed to 42°C for 2 hours and this was chosen as the standard for the cell sorting experiments. Sorting adds additional stress to the cells through shear forces and other technical manipulations which did result in a reduction of cell survival compared to unsorted cells. However, this reduction was consistent and revealed that the cells treated with HA-DESPIONs at raised temperatures were undergoing apoptotic cell death in comparison to cells treated just with hyperthermia and/or HA-DESPIONs at normal body temperature. Furthermore, experiments at 42°C showed there was a significant amount of early stage apoptotic death and late apoptotic death as well as necrosis, but there was no evidence of late apoptosis or necrosis at 40°C and 41°C. Addition of the HA-DESPIONs to cell cultures at 42°C increased overall cell death but suppressed late apoptosis and necrosis.

Given the considerable biomedical potential of nanoparticle constructs, finding multifunctional formulations that can deliver a targeted approach is an attractive goal. However, the physicochemical properties (e.g., size, surface coating, charge, and hydrophobicity) affect their physiochemical properties (toxicity and stability) of the nanoparticles and no single formulation is optimal for MRI imaging, activation by AMF, or radiosensitization. This current study demonstrates that HA-DESPIONs that are established targeted, MRI contrast agents with enhanced uptake in tumor cells are also capable of interacting with hyperthermia to induce increased cell death. We are currently working on the development of a suitable apparatus to deliver AMF to cells in culture and experimental tumors in vivo using a similar approach to Zhao and colleagues [38] and exploiting various chemical modification sites on HA (the carboxylate on the glucuronic acid, the N-acetylglucosamine hydroxyl, and the reducing end) to conjugate with drugs [32]. Drug conjugation will create a macromolecular prodrug/imaging agent where the conjugated drug becomes active upon release from the HA that will directly deliver selected agents to cancer stem cells whilst the delivery can be monitored by MRI. Activation of the hyperthermic properties of the HA-DESPIONs will add another modality to specifically target cancer stem cells.

CD44 is one of several genes, including BMI-1 [39], c-MET [40], NOTCH1 [41], ALDH1 [42], and SOX2 [43], that have been associated with poor prognosis and implicated with CSC signaling in HNSCC. There is a complex interplay between these genes which warrants further investigation in HNSCC. For instance, the combination of $CD44^{high}$ and $ALDH^{high}$ expression further identified primary HNSCC cells that showed enhanced xenotransplantation efficiency [44], the expression of NOTCH1 and β-catenin has been reported to be increased in $CD44^{high}$ HNSCC cells [45], and subpopulations of tumorigenic $CD44^{high}$ cells differentially express BMI-1 [5] which is another important CSC marker associated with self-renewal characteristics, tumor initiation, progression, invasion, metastasis, tumor recurrence, and

resistance to chemotherapy and radiotherapy in HNSCC [46]. Further work is needed to understand the interplay between stem cell-associated genes and future therapeutic strategies will necessitate a multifactorial approach to target these insidious cells.

Conflict of Interests

The authors declare that there is no conflict of interests regarding the publication of this paper.

Acknowledgments

The authors would like to thank Laura Fortier from Biobank for her generous support in flow cytometry studies. This work is funded by Department of Radiation Oncology, Beaumont Health System, and Oakland University Provost Graduate Student Research Award.

References

[1] J. B. Vermorken, E. Remenar, C. van Herpen et al., "Cisplatin, fluorouracil, and docetaxel in unresectable head and neck cancer," *The New England Journal of Medicine*, vol. 357, no. 17, pp. 1695–1704, 2007.

[2] S. C. Tremmel, K. Götte, S. Popp et al., "Intratumoral genomic heterogeneity in advanced head and neck cancer detected by comparative genomic hybridization," *Cancer Genetics and Cytogenetics*, vol. 144, no. 2, pp. 165–174, 2003.

[3] M. Bryne, M. Boysen, C. G. Alfsen et al., "The invasive front of carcinomas. the most important area for tumour prognosis?" *Anticancer Research*, vol. 18, no. 6, pp. 4757–4764, 1998.

[4] T. Reya, S. J. Morrison, M. F. Clarke, and I. L. Weissman, "Stem cells, cancer, and cancer stem cells," *Nature*, vol. 414, no. 6859, pp. 105–111, 2001.

[5] M. E. Prince, R. Sivanandan, A. Kaczorowski et al., "Identification of a subpopulation of cells with cancer stem cell properties in head and neck squamous cell carcinoma," *Proceedings of the National Academy of Sciences of the United States of America*, vol. 104, no. 3, pp. 973–978, 2007.

[6] M. Al-Hajj, M. S. Wicha, A. Benito-Hernandez, S. J. Morrison, and M. F. Clarke, "Prospective identification of tumorigenic breast cancer cells," *Proceedings of the National Academy of Sciences of the United States of America*, vol. 100, no. 7, pp. 3983–3988, 2003.

[7] S. J. Davis, V. Divi, J. H. Owen et al., "Metastatic potential of cancer stem cells in head and neck squamous cell carcinoma," *Archives of Otolaryngology—Head & Neck Surgery*, vol. 136, no. 12, pp. 1260–1266, 2010.

[8] M. C. de Jong, J. Pramana, J. E. van der Wal et al., "CD44 expression predicts local recurrence after radiotherapy in larynx cancer," *Clinical Cancer Research*, vol. 16, no. 21, pp. 5329–5338, 2010.

[9] M. Kajita, Y. Itoh, T. Chiba et al., "Membrane-type 1 matrix metalloproteinase cleaves CD44 and promotes cell migration," *Journal of Cell Biology*, vol. 153, no. 5, pp. 893–904, 2001.

[10] C. M. Isacke and H. Yarwood, "The hyaluronan receptor, CD44," *International Journal of Biochemistry & Cell Biology*, vol. 34, no. 7, pp. 718–721, 2002.

[11] M. H. El-Dakdouki, D. C. Zhu, K. El-Boubbou et al., "Development of multifunctional hyaluronan-coated nanoparticles for imaging and drug delivery to cancer cells," *Biomacromolecules*, vol. 13, no. 4, pp. 1144–1151, 2012.

[12] V. M. Plattt and F. C. Szoka Jr., "Anticancer therapeutics: targeting macromolecules and nanocarriers to hyaluronan or CD44, a hyaluronan receptor," *Molecular Pharmaceutics*, vol. 5, no. 4, pp. 474–486, 2008.

[13] T. C. Laurent, U. B. G. Laurent, and J. R. E. Fraser, "The structure and function of hyaluronan: an overview," *Immunology and Cell Biology*, vol. 74, no. 2, pp. A1–A7, 1996.

[14] A. Bartolazzi, R. Peach, A. Aruffo, and I. Stamenkovic, "Interaction between CD44 and hyaluronate is directly implicated in the regulation of tumor development," *Journal of Experimental Medicine*, vol. 180, no. 1, pp. 53–66, 1994.

[15] D. A. Gewirtz, M. L. Bristol, and J. C. Yalowich, "Toxicity issues in cancer drug development," *Current Opinion in Investigational Drugs*, vol. 11, no. 6, pp. 612–614, 2010.

[16] R. Pérez-Tomás, "Multidrug resistance: retrospect and prospects in anti-cancer drug treatment," *Current Medicinal Chemistry*, vol. 13, no. 16, pp. 1859–1876, 2006.

[17] M. M. Gottesman, T. Fojo, and S. E. Bates, "Multidrug resistance in cancer: role of ATP-dependent transporters," *Nature Reviews Cancer*, vol. 2, no. 1, pp. 48–58, 2002.

[18] M. M. Gottesman and V. Ling, "The molecular basis of multidrug resistance in cancer: the early years of P-glycoprotein research," *FEBS Letters*, vol. 580, no. 4, pp. 998–1009, 2006.

[19] D. Frank, C. Tyagi, L. Tomar et al., "Overview of the role of nanotechnological innovations in the detection and treatment of solid tumors," *International Journal of Nanomedicine*, vol. 9, no. 1, pp. 589–613, 2014.

[20] M. H. El-Dakdouki, K. El-Boubbou, D. C. Zhu, and X. Huang, "A simple method for the synthesis of hyaluronic acid coated magnetic nanoparticles for highly efficient cell labelling and in vivo imaging," *RSC Advances*, vol. 1, no. 8, pp. 1449–1452, 2011.

[21] T. Kong, J. Zeng, X. P. Wang et al., "Enhancement of radiation cytotoxicity in breast-cancer cells by localized attachment of gold nanoparticles," *Small*, vol. 4, no. 9, pp. 1537–1543, 2008.

[22] J. F. Hainfeld, D. N. Slatkin, and H. M. Smilowitz, "The use of gold nanoparticles to enhance radiotherapy in mice," *Physics in Medicine and Biology*, vol. 49, no. 18, pp. N309–N315, 2004.

[23] F.-K. Huang, W.-C. Chen, S.-F. Lai et al., "Enhancement of irradiation effects on cancer cells by cross-linked dextran-coated iron oxide (CLIO) nanoparticles," *Physics in Medicine and Biology*, vol. 55, no. 2, pp. 469–482, 2010.

[24] J. Verma, S. Lal, and C. J. F. Van Noorden, "Nanoparticles for hyperthermic therapy: synthesis strategies and applications in glioblastoma," *International Journal of Nanomedicine*, vol. 9, no. 1, pp. 2863–2877, 2014.

[25] M. Kamat, K. El-Boubbou, D. C. Zhu et al., "Hyaluronic acid immobilized magnetic nanoparticles for active targeting and imaging of macrophages," *Bioconjugate Chemistry*, vol. 21, no. 11, pp. 2128–2135, 2010.

[26] K. El-Boubbou, D. C. Zhu, C. Vasileiou et al., "Magnetic glyco-nanoparticles: a tool to detect, differentiate, and unlock the glyco-codes of cancer via magnetic resonance imaging," *Journal of the American Chemical Society*, vol. 132, no. 12, pp. 4490–4499, 2010.

[27] S. Trapasso and E. Allegra, "Role of CD44 as a marker of cancer stem cells in head and neck cancer," *Biologics*, vol. 6, pp. 379–383, 2012.

[28] D. M. Herold, I. J. Das, C. C. Stobbe, R. V. Iyer, and J. D. Chapman, "Gold microspheres: a selective technique for producing

biologically effective dose enhancement," *International Journal of Radiation Biology*, vol. 76, no. 10, pp. 1357–1364, 2000.

[29] J. C. Roeske, L. Nuñez, M. Hoggarth, E. Labay, and R. R. Weichselbaum, "Characterization of the theorectical radiation dose enhancement from nanoparticles," *Technology in Cancer Research and Treatment*, vol. 6, no. 5, pp. 395–401, 2007.

[30] G. Huang, H. Chen, Y. Dong et al., "Superparamagnetic iron oxide nanoparticles: amplifying ROS stress to improve anticancer drug efficacy," *Theranostics*, vol. 3, no. 2, pp. 116–126, 2013.

[31] S. Klein, A. Sommer, L. V. R. Distel, W. Neuhuber, and C. Kryschi, "Superparamagnetic iron oxide nanoparticles as radiosensitizer via enhanced reactive oxygen species formation," *Biochemical and Biophysical Research Communications*, vol. 425, no. 2, pp. 393–397, 2012.

[32] M. H. El-Dakdouki, E. Puré, and X. Huang, "Development of drug loaded nanoparticles for tumor targeting. Part 2: enhancement of tumor penetration through receptor mediated transcytosis in 3D tumor models," *Nanoscale*, vol. 5, no. 9, pp. 3904–3911, 2013.

[33] M. H. El-Dakdouki, K. El-Boubbou, M. Kamat et al., "CD44 targeting magnetic glyconanoparticles for atherosclerotic plaque imaging," *Pharmaceutical Research*, vol. 31, no. 6, pp. 1426–1437, 2014.

[34] S. Dutz and R. Hergt, "Magnetic particle hyperthermia—a promising tumour therapy?" *Nanotechnology*, vol. 25, no. 45, Article ID 452001, 2014.

[35] S. Dutz and R. Hergt, "Magnetic nanoparticle heating and heat transfer on a microscale: basic principles, realities and physical limitations of hyperthermia for tumour therapy," *International Journal of Hyperthermia*, vol. 29, no. 8, pp. 790–800, 2013.

[36] C. L. Dennis and R. Ivkov, "Physics of heat generation using magnetic nanoparticles for hyperthermia," *International Journal of Hyperthermia*, vol. 29, no. 8, pp. 715–729, 2013.

[37] M. Wabler, W. Zhu, M. Hedayati et al., "Magnetic resonance imaging contrast of iron oxide nanoparticles developed for hyperthermia is dominated by iron content," *International Journal of Hyperthermia*, vol. 30, no. 3, pp. 192–200, 2014.

[38] Q. Zhao, L. Wang, R. Cheng et al., "Magnetic nanoparticle-based hyperthermia for head & neck cancer in mouse models," *Theranostics*, vol. 2, no. 1, pp. 113–121, 2012.

[39] G. F. Huber, A. Albinger-Hegyi, A. Soltermann et al., "Expression patterns of Bmi-1 and p16 significantly correlate with overall, disease-specific, and recurrence-free survival in oropharyngeal squamous cell carcinoma," *Cancer*, vol. 117, no. 20, pp. 4659–4670, 2011.

[40] A. M. Baschnagel, L. Williams, A. Hanna et al., "C-met expression is a marker of poor prognosis in patients with locally advanced head and neck squamous cell carcinoma treated with chemoradiation," *International Journal of Radiation Oncology Biology Physics*, vol. 88, no. 3, pp. 701–707, 2014.

[41] D. Li, P. Dong, C. Wu, P. Cao, and L. Zhou, "Notch1 overexpression associates with poor prognosis in human laryngeal squamous cell carcinoma," *Annals of Otology, Rhinology & Laryngology*, vol. 123, no. 10, pp. 705–710, 2014.

[42] C. Zhou and B. Sun, "The prognostic role of the cancer stem cell marker aldehyde dehydrogenase 1 in head and neck squamous cell carcinomas: a meta-analysis," *Oral Oncology*, vol. 50, no. 12, pp. 1144–1148, 2014.

[43] A. Schröck, M. Bode, F. J. M. Göke et al., "Expression and role of the embryonic protein SOX2 in head and neck squamous cell carcinoma," *Carcinogenesis*, vol. 35, no. 7, pp. 1636–1642, 2014.

[44] S. Krishnamurthy, Z. Dong, D. Vodopyanov et al., "Endothelial cell-initiated signaling promotes the survival and self-renewal of cancer stem cells," *Cancer Research*, vol. 70, no. 23, pp. 9969–9978, 2010.

[45] K. Chikamatsu, H. Ishii, G. Takahashi et al., "Resistance to apoptosis-inducing stimuli in $CD44^+$ head and neck squamous cell carcinoma cells," *Head and Neck*, vol. 34, no. 3, pp. 336–343, 2012.

[46] E. Allegra, S. Trapasso, D. Pisani, and L. Puzzo, "The role of BMI1 as a biomarker of cancer stem cells in head and neck cancer: a review," *Oncology*, vol. 86, no. 4, pp. 199–205, 2014.